

Evaluation of energy absorption performance of steel square profiles with circular discontinuities

Abstract

This article details the experimental and numerical results on the energy absorption performance of square tubular profile with circular discontinuities drilled at lengthwise in the structure. A straight profile pattern was utilized to compare the absorption of energy between the ones with discontinuities under quasi-static loads. The collapse mode and energy absorption conditions were modified by circular holes. The holes were drilled symmetrically in two walls and located in three different positions along of profile length. The results showed a better performance on energy absorption for the circular discontinuities located in middle height. With respect to a profile without holes, a maximum increase of 7% in energy absorption capacity was obtained experimentally. Also, the numerical simulation confirmed that the implementation of circular discontinuities can reduce the peak load (P_{max}) by 10%. A present analysis has been conducted to compare numerical results obtained by means of the finite element method with the experimental data captured by using the testing machine. Finally the discrete model of the tube with and without geometrical discontinuities presents very good agreements with the experimental results.

Keywords

Thin walled structure, circular discontinuities, energy performance, finite element method, experimental stand.

Dariusz Szwedowicz^a
Quirino Estrada^b
Claudia Cortes^c
Jorge Bedolla^d
Gabriela Alvarez^e
Fernando Castro^f

^{a,b,c,e,f} Department of Mechanical Engineering, National Center for Research and Technological Development, Cuernavaca, Morelos, Mexico.

^d Apizaco Technological Institute, Tlaxcala, Mex.

Author email:

^ad.sz@cenidet.edu.mx

^bstrata18@cenidet.edu.mx

1 INTRODUCTION

According to a study made in 2010 the crashes from motor driven vehicles provoked more than 32 855 million deaths (DOT HS 811 552, 2012), besides an associated cost of 70 billion USD within the United States highways (Naumann and Dellinger, 2010). Because of the increase of deaths, engineers and automotive designers have tried to control the impact loads through several passive mechanisms of energy dissipation. With this purpose several devices have been proposed, however

the use of thin walled structures has started to take relevance, due to their advantages, such as simple geometries, low cost and great capacity to absorb energy by plastic deformation (Hamouda and Saied, 2007). The use of structural profiles as energy absorption devices, applied to security and protection of passengers, requires satisfying two conditions: reduction of the peak load and the maximization of the energy dissipation. With this purpose, circular (Tai and Huang, 2010), square (Abramowicz and Jones, 1984); (Aljawi, 2002), polygonal (Younes, 2009), tapered (Nagel and Thambiratnam, 2004) and double-cell tubular (Chung *et al.*, 2008) profiles, have been evaluated among others. Some works have tried to maximize the energy absorption characteristics with the implementation of friction mechanisms implicit in the interface of contact between the walls of concentric tubes, obtaining favorable results in regards to the efficiency of the force of displacement (Salehghaffari and Tajdari, 2010); (Shakeri and Salehghaffari, 2007). Another option is to modify the entire rigidity of the structure through the use of imperfections or discontinuities on the walls of the profile such as dented initiators (Lee and Hahn, 1999), dented corners (Alavi and Fallah, 2012), longitudinal grooves (Zhang and Huh, 2009), patterned windows (Song and Chen, 2013) and circular discontinuities in the sides of the tube (Arnold and Altenhoft, 2004). In all the scenarios the modifications tend to decrease the value of the peak load (Chung and Nurick, 2008); however, the deformations induced by centrally located circular hole discontinuities has demonstrated better results. Surko (1991) analyzed the theoretical behavior of the structural profiles with circular discontinuities like four plane plates with a central hole applying the concept of effective width, explained in the postulate of Von Karman. Additionally with the square profile theory developed by Abramowicz and Jones (1984), Surko (1991), an expression to calculate the strength of crushing of a particularly damaged plate was obtained. The diameter of the hole is a basic factor in magnitude of the peak load and the buckling mode or deformation. Marshall and Nurick (1998) made an experimental analysis which proved that the last load of buckling has a lineal decrease by increasing the diameter of the hole. However, an increase in the diameter causes instability in the form of buckling. Bodlani and Chung (2009a, 2009b), made a numerical and experimental analysis of the number of holes over the walls of the structure, finding a reduction of the peak load. Finally they concluded that the implementation of more than two holes in each side of the profile does not provide a better performance of the structure. Mamalis and Manolakos (2009), made a numerical and experimental analysis for the problem of localization of circular discontinuities. In their study they confirm that the reply of crushing is affected in a higher proportion by the localization of the holes in the sides of the profile more than in their diameter.

In this work the performance of steel profiles with circular discontinuities in their walls is analyzed. For this purpose experimental evaluations of steel square profiles with holes through the thickness of the walls of the profile were made, the circular discontinuities were drilled in three different positions in order to find the position that enhances the characteristics of energy absorption of the profile. The experimental results were compared with an analysis by finite elements in Abaqus, showing a good agreement.

2 EXPERIMENTAL DEVELOPMENT

The specimens were tested under quasi-static loads of compression. During the test, the profiles were placed between two plates of compression on a Shimadzu UH-300 kNI universal testing machine. The velocity of load for all cases was of 6 mm/min. The bottom plate was moved 160 mm with respect to the rigid upper compression plate. This distance corresponds to the maximum compacting distance of the tube, equivalent to 67% of the total length of the profile. Finally, the displacement-load curves were registered automatically by the system of acquisitions and data processing of the universal machine. The specimens were obtained from steel profiles with a square cross section with rounded corner (R), a nominal width (C) of 50 mm, and a thickness (t) of 1.32 mm, as shown in Figure 1. The length of the specimen (L) maintained a constant value of 240 mm in all the cases. The dimensions were determined to satisfy the geometrical relations described by Abramowicz and Jones (1986), $L/C < 10$ for $5.5 < C/t < 38$, which predict one form of symmetrical collapse of a square profile. Additionally, with the objective to ensure a uniform contact between the profile and the compression plates, the ends of the structure were machined.

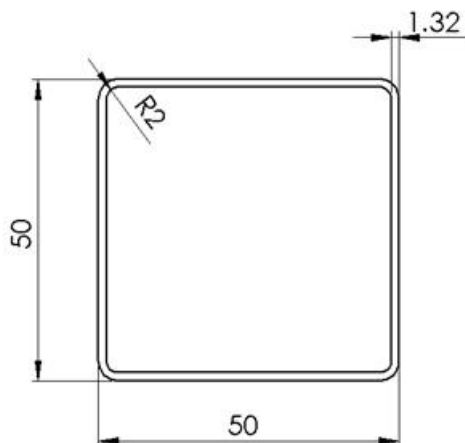


Figure 1: Geometry of a test specimen (in mm).

Taking this geometry of the profile as a pattern, circular discontinuities were placed in two opposing walls of the structure. The diameter (d) of the discontinuities was of 12 mm, and was determined from the effective width (b_e) for a thin plate based in the principle of Von Karman (Chung and Nurick, 2008; Surko, 1991).

$$b_e = 1.9t \sqrt{\frac{E}{\sigma_y}} \quad (1)$$

$$\Phi \leq C - b_e \quad (2)$$

where: C is the width of the profile, t is the wall thickness, E is the elasticity module, σ_y the yield stress, and Φ is the diameter of the hole. When the diameter (d) of the discontinuities is less than Φ the hole should have small or no effect on the buckling of the plate. Chung and Nurick (2008)

presented a study on the effect of the diameter (d) of the hole on the process of the formation of the first fold. It was found that increasing the diameter (d) the first fold is decreasing and vice versa. Also, decreasing the size of the first fold can caused instability in the buckling mode as subsequent folds formed skew. Marshall and Nurick (1998) reported this kind of the instability for 32 mm and 38 mm holes are placed in a square profile (50 mm in width, 1.2 mm in thickness, and 300 mm in length).

The holes were located in three different positions as can be observed in Figure 2 and their specifications are given in Table 1. A straight profile without discontinuities was used as a reference standard for comparison with the profiles with holes.

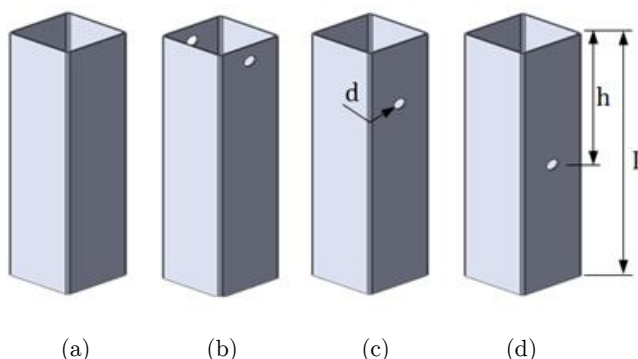


Figure 2: Longitudinal location of the holes in the specimen, where: a) ST-01 (without hole), b) DT-TOP, c) DT-QUA, d) DT-MID.

Specimen Code	Hole Diameter (d) [mm]	Position with respect to the upper end of tube (h), [mm]	Mass (m) [gr]
ST-01	No Hole	----	478.52
DT-TOP	12	15	476.18
DT-QUA	12	60	476.18
DT-MID	12	120	476.18

Table 1: Details of the specimens.

3 MEASUREMENT OF THE ENERGY ABSORPTION EFFICIENCY

Parameters that enable the evaluation of the efficiency in energy absorption in the structural profiles are presented.

In the process of crushing of the structure, the specimen reaches a peak load before starting with the plastic process folding. This force is named peak load (P_{max}) and is responsible for breaking the initial stiffness of the structure. The reduction of this parameter is a basic indicator for the use of thin - walled structures as well as for energy absorbers.

The force required for the formation of folds on the structure is called meaning load (P_m) and is given by Langseth *et al.* (1998):

$$P_m = \frac{E_a}{\delta} \quad (3)$$

where: E_a is the absorbed energy and δ is crushed displacement.

The total absorbed energy (E_a), including elastic and plastic deformations, can be calculated by the work done by the crushing force (F) on a lengthwise axial displacement (δ) using equation 1 (Chung and Nurick, 2008).

$$E_a = \int_0^{\delta} F \cdot d\delta \quad (4)$$

The amount (E_a) is represented as the area below the curve of load vs displacement and can be obtained by the trapezoidal rule, rewriting equation 1 as (Chung and Nurick, 2008):

$$E_a = \frac{1}{2} \sum_i^{n-1} (F(\delta)_{i+1} + F(\delta)_i) \cdot (\delta_{i+1} - \delta_i) \quad (5)$$

The relationship between the absorbed energy (E_a), the peak load (P_{\max}) and the displacement (δ) is known as the energetic efficiency (E_e) and is defined as (Thornton *et al.*, 1983):

$$E_e = \frac{E_a}{P_{\max} \cdot \delta} \quad (6)$$

The specific energy (S_e) is defined as the ratio of energy absorbed (E_a) to the mass (m) of the structure (Krauss and Laananen, 1994):

$$S_e = \frac{E_a}{m} \quad (7)$$

4 DEVELOPMENT AND VALIDATION OF THE NUMERICAL MODEL

The numeric results obtained in Abaqus/Explicit were validated with experimental tests. For this purpose discrete models of the problem with and without circular discontinuities were developed. The discrete model is presented in Figure 3 and consists of a profile with square cross-section and two compression rigid plates. Shell S4R elements with five integration points and a thickness of 1.32 mm were used to modeling the profile. The compression plates were modeled by four nodes R3D4 rigid elements. In addition, a mesh convergence analysis was done to determine a size of element of 3 mm for a total of 5120 elements in the profile.

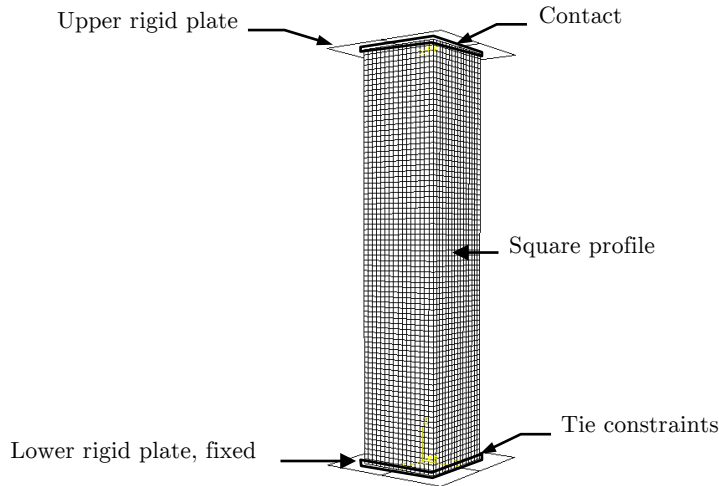


Figure 3: Discrete model and boundary conditions.

The displacement/rotation restrictions were applied on the reference nodes of the rigid bodies. The lower reference node was set fixed, while the upper compression node was restricted in all directions and rotations except in direction 2, to allow the compression of the structure. In regard to the profile, the bottom end was joined to the inferior plate of compression by a tied constraint. A contact condition was applied to the upper end of the profile, with the upper rigid compression plate. Additionally, to ensure a contact between the internal and external tube walls, a general condition contact was utilized in all model parts with a friction coefficient of 0.15.

The geometric imperfections were introduced to the model developed in Abaqus/Explicit (Abaqus, 1998) through the command *IMPERFECTION. The models were conferred with elastic-plastic characteristics of the material through an isotropic plasticity model. Material properties of the profile are defined with a Young's modulus of 200 GPa, Poisson's ratio of 0.26, yield stress of 250 MPa and material density of 7850 kg/m^3 . Due to quasi-static nature of compression test the strain rate effects were neglected.

In order to verify the congruency of the proposed discrete model to produce the plasticity phenomenon, the obtained numeric and experimental response of a profile without discontinuities was analyzed. The obtained results indicate the use feasibility of the discrete model for subsequent models with circular discontinuities. In Figure 4 the experimental and numerical collapse of the structure without imperfections is shown. The corresponding numeric and experimental graphics to the deformation and total absorbed energy are shown in Figures 5 and 6.

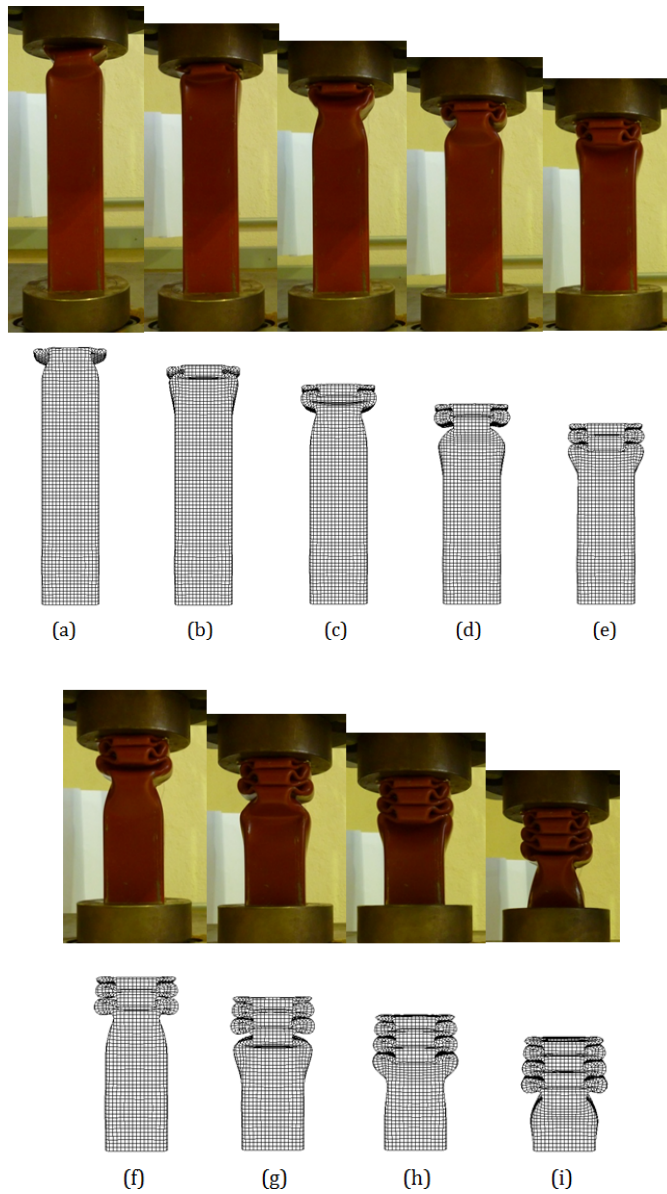


Figure 4: Experimental and numerical progressive collapse of specimen ST-01 (without holes).

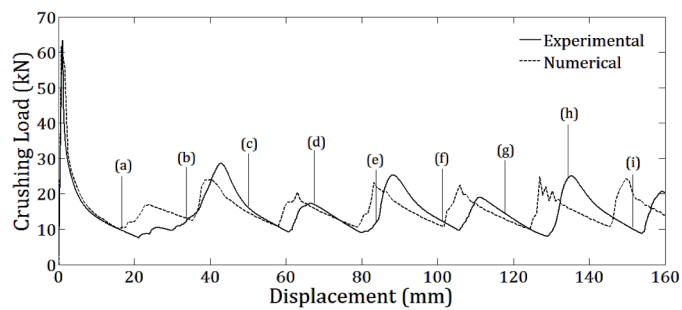


Figure 5: Comparison of numerical and experimental results for the collapse of the ST-01 specimen.

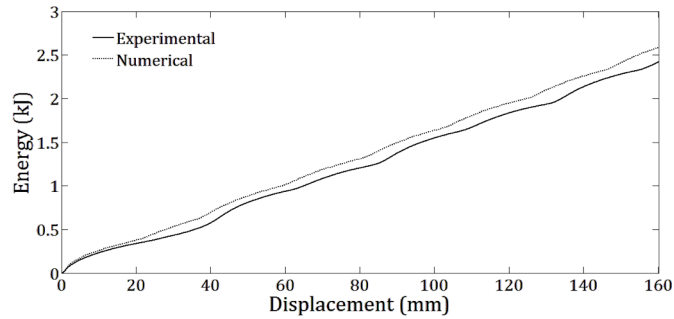


Figure 6: Energy absorbed during plastic deformation for the ST-01 specimen.

5 RESULTS AND DISCUSSION

The force vs displacement curves were obtained for each profile. It was observed that the deformation mode presented, depends in great measure, on the placement of the hole lengthwise throughout the structure. Figures 7 and 8 present the comparison of the obtained curves in experimental and numeric form in the three cases of hole placement of 12 mm (see Table 1). The load P_{\max} presents correspondence between analyses with an approximate value of 60 kN. During the plastic folding process the observed behavior is similar in the three evaluated cases (Figures 9, 11, and 13).

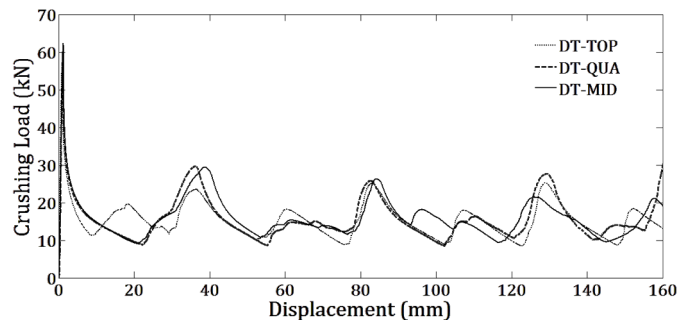


Figure 7: Load - displacement curves of specimens tested (experimental case).

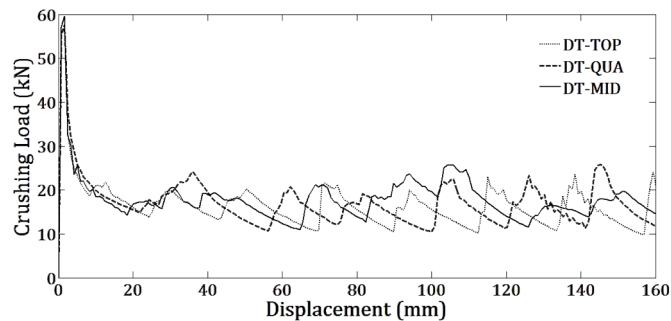


Figure 8: Load - displacement curves of specimens evaluated (numerical case).

Figures 9, 11, and 13 show the final deformation state for the specimen evaluated in the experimental and numeric analyses. Additionally, energy absorption during the crushing process is presented in Figures 10, 12, and 14, for the three different locations of the perforations.

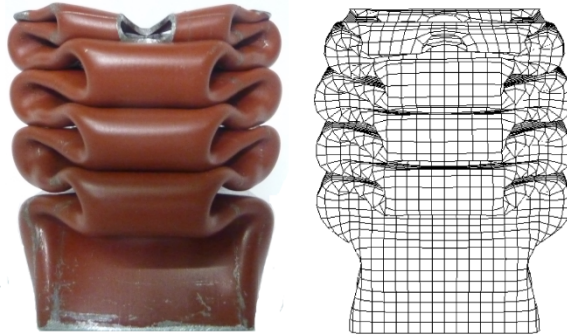


Figure 9: Final deformation state (specimen DT-TOP).

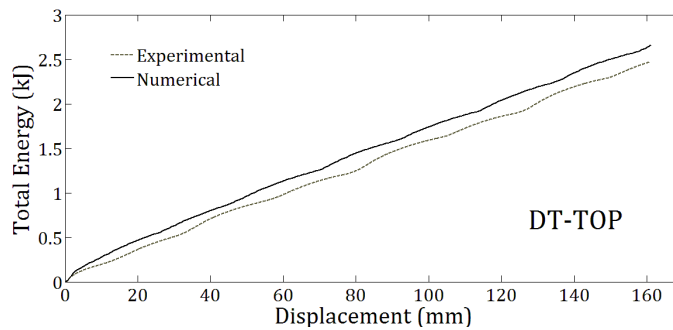


Figure 10: Absorbed energy (specimen DT-TOP).



Figure 11: Final deformation state (specimen DT-QUA).

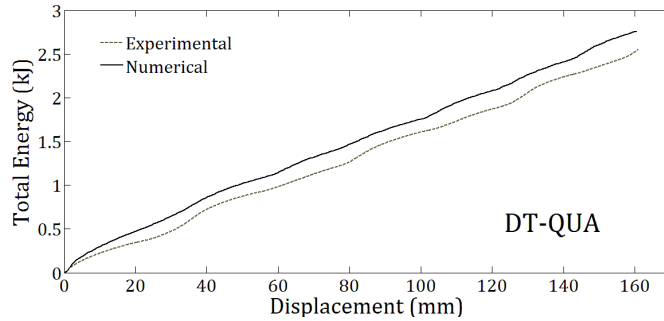


Figure 12: Absorbed energy (specimen DT-QUA).



Figure 13: Final deformation state (specimen DT-MID).

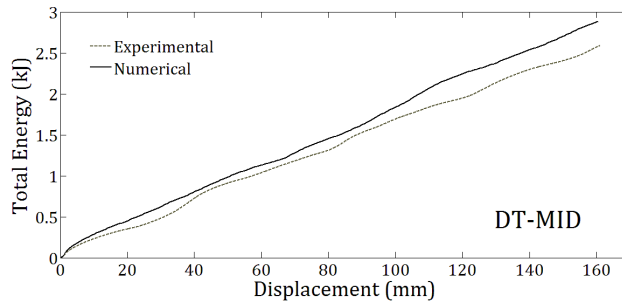


Figure 14: Absorbed energy (specimen DT-MID).

According to Abramowicz and Jones (1986, 1984), the failure modes presented in the structure were symmetrical (S), asymmetrical (A), and a combination of both (M). The implementation of circular discontinuities reduced the peak load magnitude and increased the absorption capacity of energy in respect to the ST-01 profile in all evaluated cases. Nevertheless, in accordance with the absorbed energy record graphics for each specimen, better performance was observed when placing circular discontinuities in the exact middle longitude of the structure; in this case 120 mm which corresponds to profile DT-MID. In Table 2 the comparison of the numeric and experimental results for all studied cases is presented.

Specimen	Peak load P_{max} (kN)		Meaning crushing load P_m (kN)		Total energy E_a (kJ)		Collapse mode
	Test	FEA	Test	FEA	Test	FEA	
	ST-01	63.33	61.67	15.06	16.13	2.41	
DT-TOP	57.08	56.69	15.44	16.38	2.47	2.62	S
DT-QUA	59.34	57.62	15.94	17.19	2.55	2.75	M
DT-MID	62.40	59.60	16.13	17.94	2.58	2.87	A

Table 2: Comparison of numerical (FEA) and experimental (Test) results.

The energy absorption capacity depends on the real crushing longitude of each specimen. Such a parameter indicates that profile DT-MID had a greater crushed longitude in relation to the rest of the specimens (Figure 14). For that reason an increase of area under the curve was obtained. Additionally, frictional effect may be presented on contact with the folds, as the twisting effects based on the placement of the hole in the structure; this determines its collapse mode (see Figure 15).

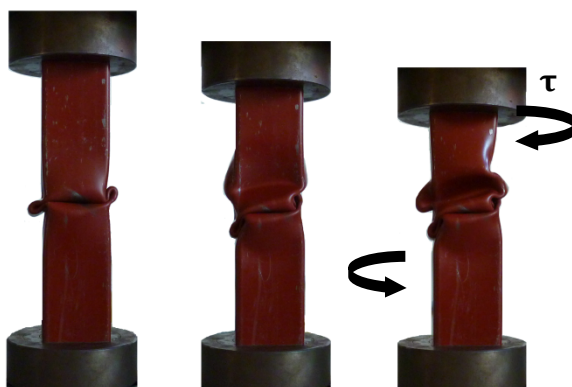


Figure 15: Torsional effects in specimen DT-MID.

The introduction of perforations in the structure modified its stiffness, causing a decrease in the peak load (P_{max}). However, its introduction causes instability and deformation mode alteration just as it was observed in specimen DT-MID. According to Abramowicz and Jones (1984) the distance (l) to which the first pleat is formed for a straight profile without discontinuities, is given depending on the thickness (t) and width of the structure (C) through the following equation:

$$\frac{l}{t} = 0.99(C/t)^{2/3} \tag{8}$$

The position of the discontinuities predefines, however, the initiation point of the formation of the first fold, continuing from this point with the process of the structure's plastic deformation (see Figure 16).

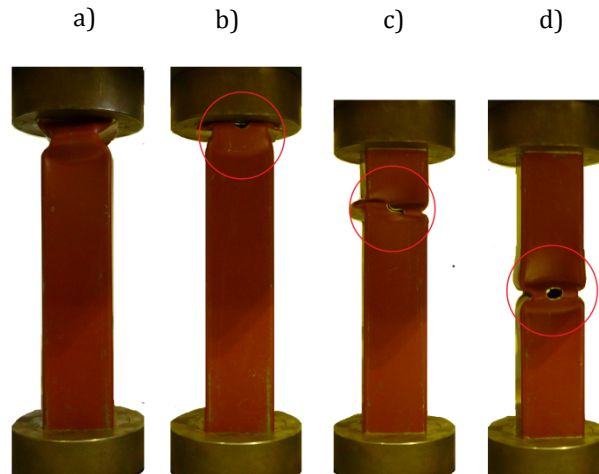


Figure 16: First fold creation, where: a) ST-01, b) DT-TOP, c) DT-QUA and d) DT-MID.

The collapse mode of the structure and the peak load value is based on the localization of the discontinuities throughout the profile. In such a way that as it furthers from any of the extremes, a transition process from a symmetrical to an asymmetrical mode of deformation is initiated. For this reason the specimens ST-01 and DT-TOP presented symmetrical failure modes, while structure DT-QUA and DT-MID presented mixed or asymmetric failure modes.

Profile DT-MID presented a better performance to the absorbed energy, but it registered a peak load (P_{\max}) value that was not the lowest compared to the other evaluated structures (see Table 2). In such manner that as the discontinuity position moves away from the top of the profile, the P_{\max} value increases.

The energetic efficiency (E_e) registered for each studied profile in numeric and experimental form, where a value equal to the unit is considered as the ideal efficiency of the system is shown in Figure 17. On this basis, the increase in the energy absorption characteristics when introducing circular discontinuities is confirmed. Numerically, DT-MID profile presented better performance ($E_e=0.30$). The numeric results present greater energetic efficiency than experimental ones due to the P_{\max} and E_a values (see Table 2).

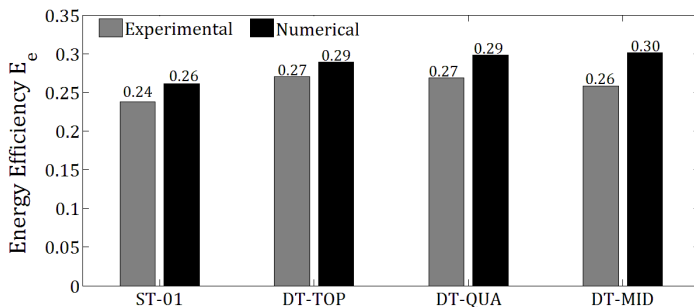


Figure 17: Comparison of the energy efficiency for all specimens.

The specific energy (S_e) was calculated for all specimens and the results are shown in Figure 18. Specimen DT-MID resulted in the largest energy absorption (J) per unit mass (gr), with a value of 5.42 and 6.00, for the experimental and the numerical studies, respectively. Determining, in this case, that in spite of the structures with discontinuities had the same mass, the location of the hole was a decisive factor in the energy absorption capacity of the profiles.

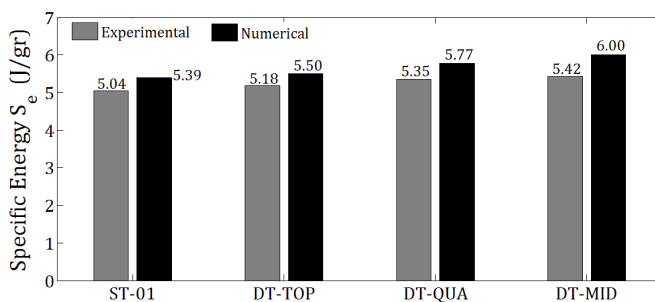


Figure 18: Comparison of the specific energy for all specimens.

5.1 Numerical analysis of the diameter of the holes

For the DT-MID specimen (see Figure 2), the influence of the diameter of the hole on the energy absorption (E_a), peak load (P_{max}) and the energetic efficiency (E_e) was analyzed. The numerically evaluated structures are shown on Table 3.

Specimen code	Hole diameter (d) [mm]	Position with respect to the upper end of tube (h), [mm]	Mass (m) [gr]
MID-03	3	120	478.38
MID-06	6	120	477.94
MID-10	10	120	476.90
MID-12	12	120	476.18
MID-16	16	120	474.36
MID-20	20	120	472.01
MID-22	22	120	470.65
MID-24	24	120	469.15

Table 3: Details of the specimens numerically evaluated.

In accordance with the obtained results, the formation of the first plastic fold of the structure was determined by the position of the holes (120 mm), thus, a magnitude dependence of P_{max} , with the size of the discontinuities, was found. During the formation of the first fold, it was observed that an excessive increase in the diameter (MID-20, MID-22 and MID-24) provokes an only partial formation of the cylindrical surfaces (E1).

On the other hand, in MID-06, MID-10, MID-12 y MID-16 structures, the hole diameter only affected the position of the hinge line and permitted the complete formation of the cylindrical surfaces (E1). In the specific case of MID-03, the effect of the diameter was almost null over the characteristics of energy absorption, and its behavior was similar to a profile without discontinuities (see Figure 19).

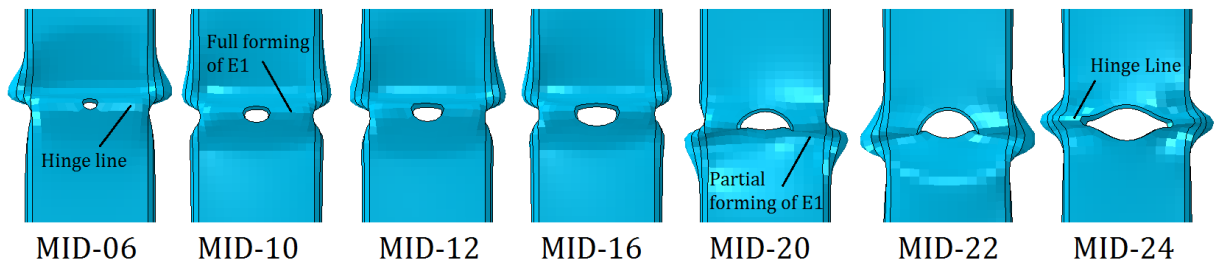


Figure 19: Effect of diameter hole on the formation of the first plastic fold of the structure.

Figure 20 shows that an increase in diameter diminishes the magnitude of the P_{max} value. The presented behavior allowed the realization of a lineal approximation, but in reaching a 20 mm diameter the value does not continue decreasing and a stabilization cycle for diameters of 22 and 24 mm is reached.

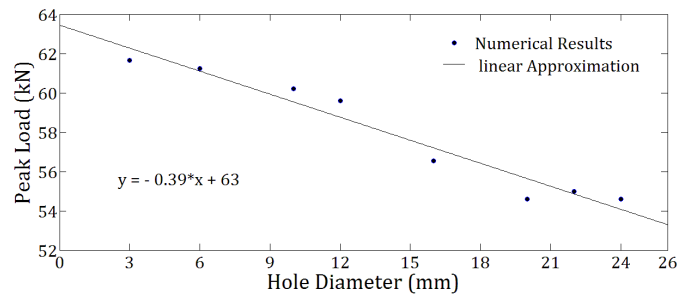


Figure 20: Effect of diameter hole on the peak load (P_{max}) for DT-MID specimen.

The total absorbed energy was obtained for each case and is presented in Figure 21. In accordance to the Von Karman principle, the value of 3 and 6 mm for diameters has a minimum effect in structure performance if compared with the absorbed energy in the profile without holes (ST-01).

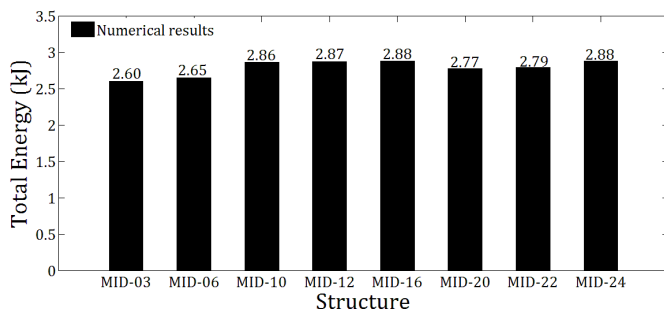


Figure 21: Total absorbed energy for different specimens to modify the diameter hole.

For the 10, 12, and 16 mm diameter values a similar performance, equivalent to the maximum energy that can be absorbed by the structure, is presented. Subsequently, a process of decrease in the performance of the structure is initiated, suggesting a limit for the sizing of the hole. The behavior described by E_a was the same which occurred when the specific energy E_e was calculated, just as is presented in Figure 22.

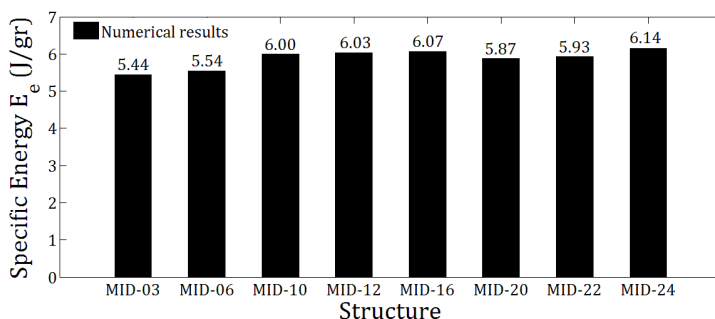


Figure 22: Total absorbed energy for different specimens to modify the diameter hole.

In this specific case, the limits related to the sizing of the holes were numerically found according to the width of structure C and the perimeter of the hole (P_b).

$$0.63C \leq P_b \leq C \quad (9)$$

6 CONCLUSIONS

This work corroborates that the implementation of circular discontinuities diminishes the value of the peak load (P_{max}) by 10 % for the DT-TOP profile. Additionally, it generates an increase in the energy absorption capacity by 7 % for the DT-MID profile. The amount of absorbed energy is based on the deformed longitude and failure mode of the profile. Despite the fact that the geometry of the profile ST-01 presented a symmetrical deformation mode, the implementation of discontinuities caused different collapse modes in the specimens DT-QUA and DT-MID. This shows that a profile with symmetric deformation mode not necessarily will have the best performance in terms of energy absorption. Numerically and experimentally it was confirmed that given the

geometric conditions of the presented specimens, the best position to implement the holes is in the middle of the structure. As the formation of the first fold takes place, not only does the energy decrease because of plastic deformation, but also and in a minor scale, losses of energy are presented due to friction and torsional effects that influence in the asymmetric or mixed deformation mode (see Figure 15). In this specific case, the limits related to the sizing of the holes were numerically found to obtain a better relationship between the absorbed energy and P_{\max} . Eventually the usefulness of the Abaqus software in the modeling process of the present problem was confirmed. In addition, a mesh convergence analysis was done to determine a size of element of 3 mm to simulate the deformation of profiles.

References

- Abaqus (1998). ABAQUS/Explicit User's Manual, Theory and examples manual and post manual. Version 5.8, Explicit, HKS, Inc.
- Abramowicz, W., Jones N., (1986). Dynamic progressive buckling of circular and square tubes. *Int. J. Impact Engineering* 4: 243-270.
- Abramowicz, W., Jones, N., (1984). Dynamic axial crushing of square tubes. *Int. J. Impact Engineering* 2:179-208.
- Alavi Nia A., Fallah Nejad Kh., (2012). Effects of buckling initiators on mechanical behavior of thin-walled square tubes subjected to oblique loading. *Thin-Walled Structures* 59: 87-96.
- Aljawi A. A. N., (2002). Axial crushing of square steel tubes. The 6th Saudi Engineering Conference, KFUPM, Dhahran 3: 3-18.
- Arnold, B., Altenhoft, W., (2004). Experimental observations on the crush characteristics of AA6061 T4 and T6 structural square tubes with and without circular discontinuities. *International Journal of Crashworthiness* 9: 73-87.
- Bodlani, S.B., Yuen Chung Kim S., Nurick, G. N., (2009a). The energy absorption characteristics of square mild steel tubes with multiple induced circular hole discontinuities-part I: Experiments. *ASME Journal of Applied Mechanics* 76: 1-11.
- Bodlani, S.B., Yuen Chung Kim S., Nurick, G. N., (2009b). The energy absorption characteristics of square mild steel tubes with multiple induced circular hole discontinuities-part II: Numerical simulations. *ASME Journal of Applied Mechanics* 76: 1-10.
- Chung Kim Yuen, S., Nurick G. N., (2008). The energy-absorbing characteristics of tubular structures with geometric and material modifications: An overview. *ASME Applied Mechanics Reviews* 61: 1-15.
- DOT HS 811 552 (2012). 2010 Motor vehicle crashed: Overview - National Highway Traffic Safety Administration U.S. Department of Transportation.
- Hamouda, A.M.S, Saied, R.O. (2007). Energy absorption capacities of square tubular structures. *Journal of Achievements in Materials and Manufacturing Engineering*, 24: 36-42.
- Krauss, C. A., Laananen, D H. (1994). A parametric study of crush initiators for a thin-walled tube. *International Journal of Vehicle Design* 15: 385-401.
- Jie Song, Yan Chen, Guoxing Lu., (2013). Light-weight thin-walled structures with patterned windows under axial crushing. *International Journal of Mechanical Sciences* 66: 239-248.
- Langseth, M., Hopperstad, O. S., Hanssen, A. G. (1998). Crash behaviour of thin-walled aluminum members. *Thin-Walled Structures* 32: 127-150.
- Lee, S., Hahn C., (1999). Effect of triggering on the energy absorption capacity of axially compressed aluminum tubes. *Mechanics and Design* 20: 31-40.

- Mamalis, A. G., Manolakos, D. E., (2009). The effect of the implementation of circular holes as crush initiators to the crushing characteristics of mild steel square tubes: Experimental and numerical simulation. *International Journal of Crashworthiness* 14: 489-501.
- Marshall, N. S., Nurick, G.N., (1998). The effect on induced imperfections on the formation of the first lobe of symmetric progressive buckling of thin-walled square tubes. *Transactions on the Built Environment* 32: 155-168.
- Nagel, G. M., Thambiratnam, D. P., (2004). A numerical study on the impact response and energy absorption of tapered thin-walled tubes. *International Journal of Mechanics Sciences* 46: 201-216.
- Naumann, B. R., Dellinger, M. A. (2010). Incidence and total lifetime costs of motor vehicle-related fatal and nonfatal injury by road user type, United States, 2005, *Traffic Injury Prevention* 11: 353-360.
- Chung, S. K. Y., Nurick, G.N., Starke R.A., (2008). The energy absorption characteristics of double-cell tubular profiles, *Latin American Journal of Solids and Structures* 5: 289-317.
- Salehghaffari, S., Tajdari, M., (2010). Attempts to improve energy absorption characteristics of circular metal tubes subjected to axial loading. *Thin Walled Structures* 48: 379-390.
- Shakeri, M., Salehghaffari, S., (2007). Expansion of circular tubes by rigid tubes as impact energy absorbers: experimental and theoretical investigation. *International Journal of Crashworthiness TCR* 12: 493-501.
- Surko, S. W., (1991). Crushing strength of box columns with partially damaged plating. *Int. J. Mech. Sci.* 33: 1017-1028.
- Tai, Y.S., Huang, M. Y. (2010). Axial compression and energy absorption characteristics of high-strength thin walled cylinders under impact load. *Theoretical and Applied Fracture Mechanics* 53: 1-8.
- Thornton, P. H., Mahmood, H. F., and Magee, C. L., (1983). Energy absorption by structural collapse. *Structural Crashworthiness*, Butterworths, London, 96–117.
- Younes, M. M., (2009). Finite element modeling of crushing behavior of thin tubes with various cross-sections. 13th International Conference on Aerospace Sciences & Aviation Technology, ASAT-13, Paper: ASAT-13-ST-34.
- Zhang, X., Huh H., (2009). Energy absorption of longitudinally grooved square tubes under axial compression. *Thin walled-Walled Structures* 47: 1469-1477.